

Processes of $e^+e^- \rightarrow [\eta, \eta', \eta(1295), \eta(1405)]\gamma$ in the extended Nambu–Jona-Lasinio model

A. I. Ahmadov,^{1,2,*} D. G. Kostunin,^{3,†} and M. K. Volkov^{1,‡}

¹*Bogoliubov Laboratory of Theoretical Physics, JINR, Dubna 141980 Russia*

²*Institute of Physics, Azerbaijan National Academy of Science, Baku, Azerbaijan*

³*Institut für Kernphysik, Karlsruhe Institute of Technology (KIT), Karlsruhe, Germany*

(Received 13 March 2013; published 11 April 2013)

In the extended Nambu–Jona-Lasinio (NJL) model the total cross sections of the processes $e^+e^- \rightarrow [\eta, \eta', \eta(1295), \eta(1405)]\gamma$ at energies up to 2 GeV are calculated. The intermediate vector mesons $\rho(770)$, $\omega(782)$, $\phi(1020)$, $\rho'(1450)$, $\omega'(1420)$, and $\phi'(1680)$ are taken into account. The latter three mesons are treated as the first radial excited states. They are incorporated into the NJL model by means of polynomial form factors. The calculation results are in satisfactory agreement with the experimental data obtained with the SND detector at VEPP-2M, Novosibirsk. The predictions given for the process $e^+e^- \rightarrow [\eta', \eta(1295), \eta(1405)]\gamma$ have not been experimentally tested yet.

DOI: [10.1103/PhysRevC.87.045203](https://doi.org/10.1103/PhysRevC.87.045203)

PACS number(s): 12.39.Fe, 13.20.Jf, 13.66.Bc, 24.85.+p

I. INTRODUCTION

Recently in Refs. [1–5], it has been shown that in the framework of the extended chiral Nambu–Jona-Lasinio (NJL) model [6–8] the $e^+e^- \rightarrow [\pi^0, \pi^{0'}(1300)]\gamma$, $\pi[\pi, \pi'(1300)]$, $\pi^0\omega$, and $\pi^0\rho^0$ processes are satisfactorily described at energies up to 1.6 GeV. The contributions from the intermediate vector mesons in both the ground and radially excited states were taken into account. Radially excited states of mesons were introduced in the standard NJL model with the polynomial form factor of the second order in the transverse momentum of quarks [6–8]. In this case, the slope parameter of this form factor was defined by the condition that the quark condensate did not change after the introduction of excited meson states in the standard NJL model. In contrast with other phenomenological models used for description of low-energy interactions of mesons, the extended NJL model does not need to introduce additional arbitrary parameters for the above processes (see, for instance, [9,10]). Up to now the processes with pion production, as well as ρ , ω , and γ in the final state, have been considered. To do this, it was sufficient to use the $SU(2) \times SU(2)$ NJL model. To consider the processes with production of η and η' mesons in the final state, one has to use the extended $U(3) \times U(3)$ NJL model. In Ref. [11], the photoproduction of $\eta(550)$, $\eta'(950)$, $\eta(1295)$, and $\eta(1405)$ in colliding electron-positron beams was studied. Unlike the previous works, here we had to use the mixing matrix of the four isoscalar states of η mesons [12].

In this work, we will continue investigation in this direction; namely, we will calculate the total cross section of the processes $e^+e^- \rightarrow [\eta, \eta', \eta(1295), \eta(1405)]\gamma$, with intermediate states of vector mesons, in both the ground and radial-excited states in the energy region up to 2 GeV. Our results for the process $e^+e^- \rightarrow \eta\gamma$ are in satisfactory agreement with the experimental data obtained in Ref. [13]. The predictions for

the processes containing η' , $\eta(1295)$, and $\eta(1405)$ are given. The predictions can be verified in the ongoing experiment at VEPP-2000 (Novosibirsk).

II. LAGRANGIAN OF THE EXTENDED NJL MODEL

In Figs. 1 and 2 the processes $e^+e^- \rightarrow (\eta, \eta', \hat{\eta}, \hat{\eta}')\gamma$ taking into account intermediate particles γ , ρ , ω , ϕ , ρ' , ω' , and ϕ' are given.

For the description of these processes we will use the lagrangian of the extended $U(3) \times U(3)$ NJL model [12,14,15],

$$\begin{aligned} \Delta\mathcal{L}_2^{\text{int}} &= \bar{q}(k')(L_f + L_\gamma + L_V + L_{\eta,\eta',\hat{\eta},\hat{\eta}'})q(k), \\ L_f &= i\hat{\partial} - m, \\ L_\gamma &= \frac{e}{2} \left(\lambda_3 + \frac{\lambda_8}{\sqrt{3}} \right) \hat{A}, \\ L_V &= A_{\omega,\rho}[\lambda_3\hat{\rho}(p) + \lambda_u\hat{\omega}(p)] + A_\phi\lambda_s\hat{\phi}(p) \\ &\quad - A_{\omega',\rho'}[\lambda_3\hat{\rho}'(p) + \lambda_u\hat{\omega}'(p)] - A_{\phi'}\lambda_s\hat{\phi}'(p), \\ L_{\eta,\eta',\hat{\eta},\hat{\eta}'} &= i\gamma_5 \sum_{q=u,s} \lambda_q \sum_{\eta=\eta,\eta',\hat{\eta},\hat{\eta}'} A_\eta^q \eta(p), \end{aligned} \quad (1)$$

where $\bar{q} = (\bar{u}, \bar{d}, \bar{s})$ with u , d , and s quark fields; $m = \text{diag}(m_u, m_d, m_s)$, $m_u = m_d = 280$ MeV, and $m_s = 455$ MeV are the constituent quark masses; e is the electron charge; A is the photon field; ρ , ω , ϕ , η , η' , $\hat{\eta}$, and $\hat{\eta}'$ are meson fields (a hat over η or η' fields means an excited state); and

$$\begin{aligned} \lambda_3 &= \begin{pmatrix} 1 & & \\ & -1 & \\ & & 0 \end{pmatrix}, \quad \lambda_8 = \frac{1}{\sqrt{3}} \begin{pmatrix} 1 & & \\ & 1 & \\ & & -2 \end{pmatrix}, \\ \lambda_u &= \begin{pmatrix} 1 & & \\ & 1 & \\ & & 0 \end{pmatrix}, \quad \lambda_s = \begin{pmatrix} 1 & & \\ & 1 & \\ & & \sqrt{2} \end{pmatrix}, \\ A_{\omega,\rho} &= g_{\rho_1} \frac{\sin(\beta^u + \beta_0^u)}{\sin(2\beta_0^u)} + g_{\rho_2} f_u(k^{\perp 2}) \frac{\sin(\beta^u - \beta_0^u)}{\sin(2\beta_0^u)}, \\ A_{\omega',\rho'} &= g_{\rho_1} \frac{\cos(\beta^u + \beta_0^u)}{\sin(2\beta_0^u)} + g_{\rho_2} f_u(k^{\perp 2}) \frac{\cos(\beta^u - \beta_0^u)}{\sin(2\beta_0^u)}, \end{aligned} \quad (2)$$

*ahmadov@theor.jinr.ru

†dmitriy.kostunin@kit.edu, kostunin@theor.jinr.ru

‡volkov@theor.jinr.ru

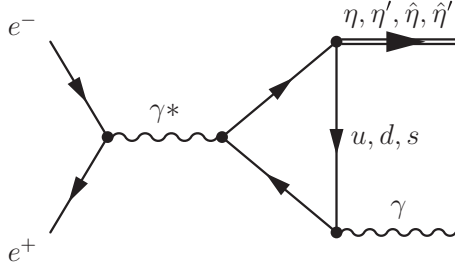


FIG. 1. Feynman diagram with photon exchange.

$$A_\phi = g_{\phi_1} \frac{\sin(\beta^s + \beta_0^s)}{\sin(2\beta_0^s)} + g_{\phi_2} f_s(k^\perp{}^2) \frac{\sin(\beta^s - \beta_0^s)}{\sin(2\beta_0^s)},$$

$$A_{\phi'} = g_{\phi_1} \frac{\cos(\beta^s + \beta_0^s)}{\sin(2\beta_0^s)} + g_{\phi_2} f_s(k^\perp{}^2) \frac{\cos(\beta^s - \beta_0^s)}{\sin(2\beta_0^s)}, \quad (3)$$

$$A_{\eta, \hat{\eta}, \eta', \hat{\eta}'}^q = g_{q_1} b_{\eta, \hat{\eta}, \eta', \hat{\eta}'}^{\varphi_{q,1}} + g_{q_2} b_{\eta, \hat{\eta}, \eta', \hat{\eta}'}^{\varphi_{q,2}} f_u(k^\perp{}^2), \quad (4)$$

where $q = u, s$. The radially excited states were represented in the NJL model using the form factor in the quark-meson interaction,

$$f_q(k^\perp{}^2) = (1 - d_q |k^\perp{}^2|) \Theta(\Lambda_3^2 - |k^\perp{}^2|),$$

$$k^\perp = k - \frac{(kp)p}{p^2}, \quad d_u = 1.788 \text{ GeV}^{-2}, \quad (5)$$

$$d_s = 1.727 \text{ GeV}^{-2},$$

where k and p are the quark and meson momenta, respectively. The cutoff parameter $\Lambda_3 = 1.03 \text{ GeV}$. The coupling constants are defined in the extended NJL model by the integrals containing given form-factors,

$$g_{q_1} = \left(4 \frac{I_2(m_q)}{Z_q}\right)^{-1/2}, \quad g_{q_2} = (4I_2^{f^2}(m_q))^{-1/2},$$

$$g_{\rho_1} = \left(\frac{2}{3} I_2(m_u)\right)^{-1/2}, \quad g_{\rho_2} = \left(\frac{2}{3} I_2^{f^2}(m_u)\right)^{-1/2}, \quad (6)$$

$$g_{\phi_1} = \left(\frac{2}{3} I_2(m_s)\right)^{-1/2}, \quad g_{\phi_2} = \left(\frac{2}{3} I_2^{f^2}(m_s)\right)^{-1/2},$$

where the Z_q factor appeared after taking into account pseudoscalar-axial-vector transitions, $Z_s \approx Z_u = 1.2$,

$$I_m^{f^n}(m_q) = -i N_c \int \frac{d^4 k}{(2\pi)^4} \frac{[f_q(k^\perp{}^2)]^n}{(m_q^2 - k^2)^m} \Theta(\Lambda_3^2 - \vec{k}^2), \quad (7)$$

where $N_c = 3$ is a number of quark colors. The mixing angles for vector mesons are $\beta_0^u = 61.44^\circ$, $\beta^u = 79.85^\circ$,

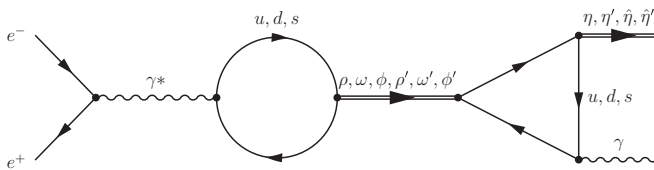

FIG. 2. Feynman diagrams with ρ , ω , ϕ , ρ' , ω' , and ϕ' meson exchange.

TABLE I. The mixing coefficients for the isoscalar pseudoscalar meson states.

| | η | $\hat{\eta}$ | η' | $\hat{\eta}'$ |
|-----------------|--------|--------------|---------|---------------|
| $\varphi_{u,1}$ | 0.71 | 0.62 | -0.32 | 0.56 |
| $\varphi_{u,2}$ | 0.11 | -0.87 | -0.48 | -0.54 |
| $\varphi_{s,1}$ | 0.62 | 0.19 | 0.56 | -0.67 |
| $\varphi_{s,2}$ | 0.06 | -0.66 | 0.30 | 0.82 |

$\beta_0^s = 57.11^\circ$, and $\beta^s = 76.18^\circ$. One can find the definition of mixing angles for ρ , ω , and ϕ mesons in Refs. [12,14]. The mixing coefficients for the isoscalar pseudoscalar meson states given in Table I were defined in Ref. [15].

It should be noted that meson states $\phi'(1680)$ are taken into account only for qualitative predictions because their mass is very close to the masses of $\rho''(1690)$ and $\omega''(1670)$, which are not described in the framework of our version of the extended NJL model.

III. AMPLITUDES AND CROSS SECTIONS OF THE PROCESSES

All amplitudes of the given processes have the form

$$T^\lambda = \bar{e} \gamma^\mu e \frac{p_\eta^\alpha p_\gamma^\beta}{ms} \{T_\gamma + T_{\rho+\omega} + T_\phi + T_{\rho'+\omega'} + T_{\phi'}\} \varepsilon_{\mu\lambda\alpha\beta}, \quad (8)$$

where $s = (p_+(e^+) + p_-(e^-))^2$. The contributions from the photon and vector mesons read

$$T_\gamma = \frac{2}{3} \left(5 \frac{16}{3} \pi^2 m_u V_{\gamma u} + \sqrt{2} \frac{16}{3} \pi^2 m_s V_{\gamma s}\right),$$

$$T_{\rho+\omega} = \left(\frac{3s}{m_\rho^2 - s - i\sqrt{s}\Gamma_\rho} + \frac{1}{3} \frac{s}{m_\omega^2 - s - i\sqrt{s}\Gamma_\omega}\right) \times \frac{C_{\gamma\rho}}{g_{\rho_1}} \left(\frac{16}{3} \pi^2 m_u V_\rho\right),$$

$$T_\phi = -\frac{2\sqrt{2}}{3} \frac{s}{m_\phi^2 - s - i\sqrt{s}\Gamma_\phi} \frac{C_{\gamma\phi}}{g_{\phi_1}} \left(\frac{16}{3} \pi^2 m_s V_\phi\right), \quad (9)$$

$$T_{\rho'+\omega'} = \left(\frac{3s}{m_{\rho'}^2 - s - i\sqrt{s}\Gamma_{\rho'}(s)} + \frac{1}{3} \frac{s}{m_{\omega'}^2 - s - i\sqrt{s}\Gamma_{\omega'}(s)}\right) \times \frac{C_{\gamma\rho'}}{g_{\rho_1}} \left(\frac{16}{3} \pi^2 m_u V_{\rho'}\right) e^{i\pi},$$

$$T_{\phi'} = -\frac{2\sqrt{2}}{3} \frac{s}{m_{\phi'}^2 - s - i\sqrt{s}\Gamma_{\phi'}} \frac{C_{\gamma\phi'}}{g_{\phi_1}} \left(\frac{16}{3} \pi^2 m_s V_{\phi'}\right),$$

where the coefficients $C_{\gamma V}$ denote the transitions of a photon into vector mesons,

$$C_{\gamma V_q} = \frac{\sin(\beta^q + \beta_0^q)}{\sin(2\beta_0^q)} + \Gamma_q \frac{\sin(\beta^q - \beta_0^q)}{\sin(2\beta_0^q)},$$

$$C_{\gamma V'_q} = -\left(\frac{\cos(\beta^q + \beta_0^q)}{\sin(2\beta_0^q)} + \Gamma_q \frac{\cos(\beta^q - \beta_0^q)}{\sin(2\beta_0^q)}\right),$$

$$\Gamma_q = \frac{I_2^f(m_q)}{\sqrt{I_2(m_q)I_2^{f^2}(m_q)}}, \quad \Gamma_u = 0.54, \quad \Gamma_s = 0.41,$$

$$q = u, s, \quad V_u = \rho, \quad V_u' = \rho', \quad V_s = \phi, \quad V_s' = \phi'. \quad (10)$$

The values of the triangles $V_{\gamma, \rho, \phi, \rho', \phi'} = V_{\gamma, \rho, \phi, \rho', \phi'}^{\eta, \eta', \hat{\eta}, \hat{\eta}'}$ depend on the outgoing particles. We give their values:

$$V_{\gamma q}^{\eta, \eta', \hat{\eta}, \hat{\eta}'} = \sum_{i=1,2} b_{\eta, \hat{\eta}, \eta', \hat{\eta}'}^{\varphi_{q,i}} g_{q_i} I_3(m_q),$$

$$V_{V_q}^{\eta, \eta', \hat{\eta}, \hat{\eta}'} = \frac{\sin(\beta^q + \beta_0^q)}{\sin(2\beta_0^q)} b_{\eta, \hat{\eta}, \eta', \hat{\eta}'}^{\varphi_{q,1}} g_{V_1} g_{q_1} I_3(m_q)$$

$$+ \frac{\sin(\beta^q - \beta_0^q)}{\sin(2\beta_0^q)} b_{\eta, \hat{\eta}, \eta', \hat{\eta}'}^{\varphi_{q,1}} g_{V_2} g_{q_1} I_3^f(m_q)$$

$$+ \frac{\sin(\beta^q + \beta_0^q)}{\sin(2\beta_0^q)} b_{\eta, \hat{\eta}, \eta', \hat{\eta}'}^{\varphi_{q,2}} g_{V_1} g_{q_2} I_3^f(m_q)$$

$$+ \frac{\sin(\beta^q - \beta_0^q)}{\sin(2\beta_0^q)} b_{\eta, \hat{\eta}, \eta', \hat{\eta}'}^{\varphi_{q,2}} g_{V_2} g_{q_2} I_3^f(m_q),$$

$$-V_{V_q'}^{\eta, \eta', \hat{\eta}, \hat{\eta}'} = \frac{\cos(\beta^q + \beta_0^q)}{\sin(2\beta_0^q)} b_{\eta, \hat{\eta}, \eta', \hat{\eta}'}^{\varphi_{q,1}} g_{V_1} g_{q_1} I_3(m_q)$$

$$+ \frac{\cos(\beta^q - \beta_0^q)}{\sin(2\beta_0^q)} b_{\eta, \hat{\eta}, \eta', \hat{\eta}'}^{\varphi_{q,1}} g_{V_2} g_{q_1} I_3^f(m_q)$$

$$+ \frac{\cos(\beta^q + \beta_0^q)}{\sin(2\beta_0^q)} b_{\eta, \hat{\eta}, \eta', \hat{\eta}'}^{\varphi_{q,2}} g_{V_1} g_{q_2} I_3^f(m_q)$$

$$+ \frac{\cos(\beta^q - \beta_0^q)}{\sin(2\beta_0^q)} b_{\eta, \hat{\eta}, \eta', \hat{\eta}'}^{\varphi_{q,2}} g_{V_2} g_{q_2} I_3^f(m_q). \quad (11)$$

For the ρ' meson we use the width $\Gamma_{\rho'}(s)$ similar to Ref. [4],

$$\Gamma_{\rho'}(s) = \Theta(2m_\pi - \sqrt{s})\Gamma_{\rho' \rightarrow 2\pi}$$

$$+ \Theta(\sqrt{s} - 2m_\pi) \left(\Gamma_{\rho' \rightarrow 2\pi} + \Gamma_{\rho' \rightarrow \omega\pi} \frac{\sqrt{s} - 2m_\pi}{m_\omega - m_\pi} \right)$$

$$\times \Theta(m_\omega + m_\pi - \sqrt{s})$$

$$+ \Theta(m_{\rho'} - \sqrt{s})\Theta(\sqrt{s} - m_\omega - m_\pi)$$

$$\times \left(\Gamma_{\rho' \rightarrow 2\pi} + \Gamma_{\rho' \rightarrow \omega\pi} + (\Gamma_{\rho'} - \Gamma_{\rho' \rightarrow 2\pi} - \Gamma_{\rho' \rightarrow \omega\pi}) \right)$$

$$\times \frac{\sqrt{s} - m_\omega - m_\pi}{m_{\rho'} - m_\omega - m_\pi} \Big) + \Theta(\sqrt{s} - m_{\rho'})\Gamma_{\rho'}, \quad (12)$$

where $\Gamma_{\rho' \rightarrow 2\pi} = 22$ MeV and $\Gamma_{\rho' \rightarrow \omega\pi} = 75$ MeV were calculated in Ref. [14]; we use the complete width $\Gamma_{\rho'} = 400$ MeV [16]. For the widths of ω' and ϕ' mesons in Breit-Wigner formulas we will use the more simple expression for the width of their decays. Namely we will use ω' and ϕ' decays width value at $\sqrt{s} = m_{\omega', \phi'}$. This is justified by the fact that the contribution of the amplitude of the intermediate ω' mesons is an order of magnitude lower than the contribution from the amplitude of the ρ' in the intermediate state. As for the ϕ' meson, its contribution is significant only in the region $\sqrt{s} > 1.5$ GeV. For other mesons we use static widths. For all masses and decay widths we used the standard PDG values [16]. Let us note that the ρ' and ω' mesons have similar masses and decay widths and $T_{\omega'} \approx 0.1 T_{\rho'}$. That means that the

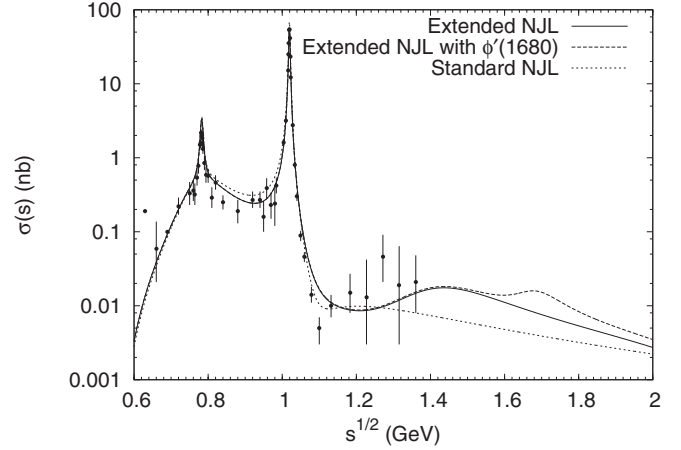


FIG. 3. Comparison of the NJL model predictions with the experiment [13] for the $e^+e^- \rightarrow \eta\gamma$ process.

contribution from the ω' meson to the cross section is negligible in the present processes. Unfortunately, our model cannot describe phases of the excited intermediate resonances, thus we take the phases for ρ' and ω' from the experiments [3,13], $T_{\rho', \omega'} \rightarrow e^{i\pi} T_{\rho', \omega'}$.

The total cross section takes the form

$$\sigma(s) = \frac{\alpha}{24\pi^2 s^3} \lambda^{3/2}(s, m, 0) |T|^2, \quad (13)$$

where $\lambda(a, b, c) = (a - b - c)^2 - 4bc$, $m = m_\eta, m_{\eta'}, m_{\hat{\eta}}, m_{\hat{\eta}'}$. One can find the cross sections of each of four processes in Figs. 3–6. We calculated every cross section up to 2 GeV, and give a comparison with experiment in Fig. 3 (experimental points shown in Fig. 3 are taken from Ref. [13]) and three predictions for each process involving η' , $\eta(1295)$, and $\eta(1405)$ mesons (see Figs. 4–6). Every process was calculated with several different amplitudes. The first amplitude was calculated in the extended NJL model but without the contribution of the ϕ' meson (solid curves). The second amplitude was obtained from the same amplitudes taking into account contribution $T_{\phi'}$ from the ϕ' meson (dashed curves). The third amplitude (in Figs. 3 and 4) was obtained in the framework

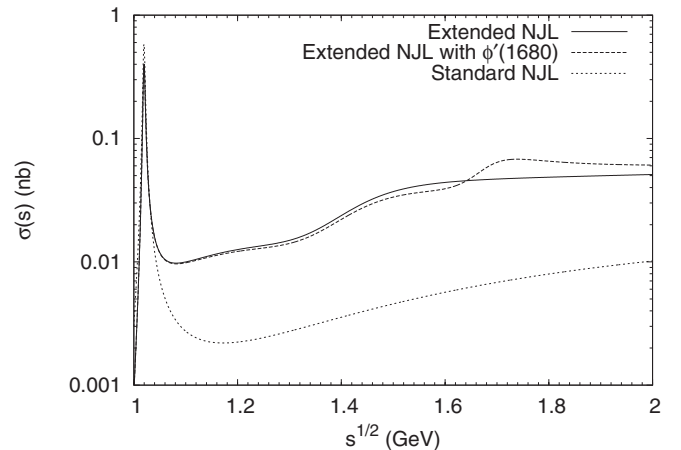


FIG. 4. Predictions for the $e^+e^- \rightarrow \eta'\gamma$ process given by the extended and standard NJL models.

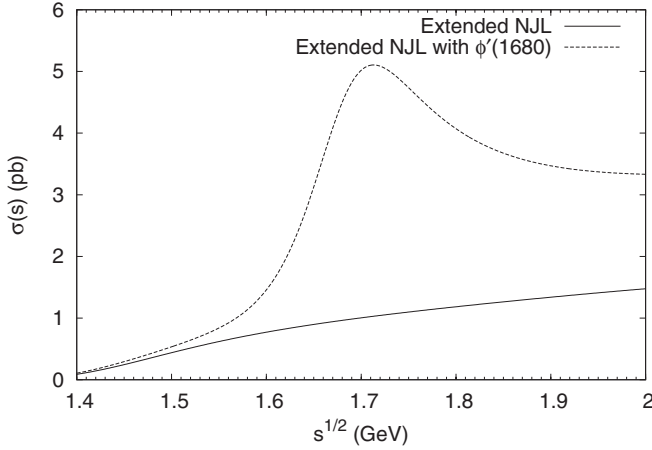


FIG. 5. Predictions for the $e^+e^- \rightarrow \eta(1295)\gamma$ process given by the extended NJL model.

of the standard NJL model (dotted curves). Note that in Fig. 3 one can see two sharp peaks. The first peak corresponds to the ρ and ω intermediate resonant contributions, the second one is due to the ϕ meson.

One can see that heavier resonances like $\phi'(1680)$ may play a significant role after 1.5 GeV, especially in processes with outgoing particles heavier than 1.2 GeV (see Figs. 5 and 6).

IV. CONCLUSION

The calculations resulted in satisfactory agreement with the experimental data relating to the measurement of the $e^+e^- \rightarrow \eta\gamma$ process in the energy region 0.6–1.4 GeV. The contributions of the intermediate vector mesons ρ , ω , ϕ , ρ' , ω' , and ϕ' were taken into account. For the calculations of processes involving ground and excited states of the intermediate vector resonances, we used the extended NJL model.

We demonstrate that the contributions of the amplitudes with the intermediate ρ , ω , and ϕ mesons in the ground states give results very close to the ones obtained within the extended model up to about 1.5 GeV, where the ρ' resonance contribution becomes important.

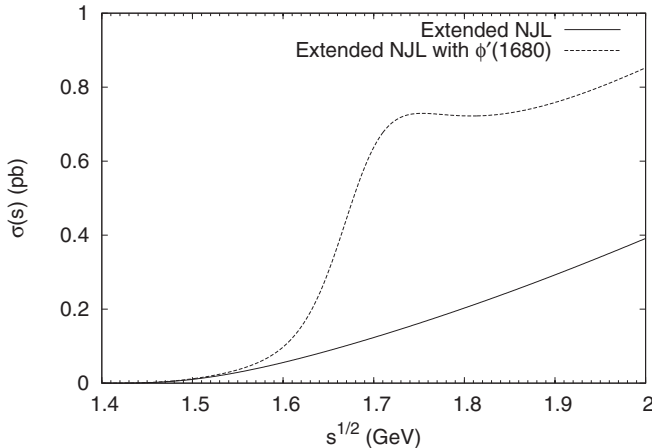


FIG. 6. Predictions for the $e^+e^- \rightarrow \eta(1405)\gamma$ process given by the extended NJL model.

It should be emphasized that our version of the extended model contains only the ground and the first radially excited states of the vector mesons.

We introduced radially excited $\phi'(1680)$ to show that heavier resonances like this one can make a notable contribution to cross sections at larger energies.

In the reactions considered here, the main role is played by processes with intermediate vector mesons. However, there are also reactions where intermediate scalar, tensor, and axial-vector mesons do contribute as well; see, e.g., Refs. [17–19].

We hope that our predictions for production of final states with η' , $\eta(1295)$, and $\eta(1405)$ will be experimentally verified in existing and future experiments at e^+e^- colliders.

ACKNOWLEDGMENT

We are grateful to A. B. Arbuzov, E. A. Kuraev and V. V. Lenok for useful discussions.

APPENDIX: CALCULATIONS WITHIN THE STANDARD NJL MODEL

In this Appendix, we will show the calculation of the amplitude of the process $e^+e^- \rightarrow \eta\gamma$ in the framework of the standard NJL model. The Lagrangian of the standard NJL model has the form [15,20–22]

$$\begin{aligned} \mathcal{L}_{\text{standard}}^{\text{int}} = & \bar{q} \left[i \hat{\partial} - m + \frac{e}{2} \left(\lambda_3 + \frac{\lambda_8}{\sqrt{3}} \right) \hat{A} \right. \\ & + i \gamma_5 \eta (\lambda_u g_\pi \sin \bar{\theta} + \lambda_s g_s \cos \bar{\theta}) \\ & + i \gamma_5 \eta' (\lambda_u g_\pi \cos \bar{\theta} - \lambda_s g_s \sin \bar{\theta}) \\ & \left. + \frac{g_\rho}{2} (\lambda \hat{\rho} + \lambda_u \hat{\omega}) + \frac{g_\phi}{2} \lambda_s \hat{\phi} \right] q, \end{aligned} \quad (\text{A1})$$

where $\bar{\theta} = \theta - \theta_0 = -54^\circ$, θ is the singlet-octet mixing angle, and θ_0 is the ideal mixing angle; the coupling constants are $g_\pi = g_{u_1} = m_u/F_\pi$, $F_\pi = 93$ MeV, $g_\rho = g_{\rho_1}$, $g_s = g_{s_1}$, and $g_\phi = g_{\phi_1}$.

One can find the description of the transition of a photon into vector mesons into Ref. [20]. The amplitudes of the decays ρ , ω , ϕ were calculated in Ref. [21]. We will follow the standard model and calculate convergent integrals which contain three quark propagators within the infinite limits:

$$\begin{aligned} I_3^{(\infty)}(m_q) &= \frac{16}{3} \pi^2 m_q I_3(m_q) \Big|_{\Lambda_3 \rightarrow \infty} \\ &= \int \frac{d^4 k}{i \pi^2} \frac{m_q}{(m_q^2 - k^2)^3} = \frac{1}{2m_q}. \end{aligned} \quad (\text{A2})$$

Thus, the amplitude T_{standard} for the given process contains the following terms:

$$\begin{aligned} T_\gamma &= \frac{1}{3} \left(5 \frac{g_\pi \sin \bar{\theta}}{m_u} + \sqrt{2} \frac{g_s \cos \bar{\theta}}{m_s} \right), \\ T_{\rho+\omega} &= \frac{g_\pi}{2m_u} \left(\frac{3s}{m_\rho^2 - s - i\sqrt{s}\Gamma_\rho} + \frac{1}{3} \frac{s}{m_\omega^2 - s - i\sqrt{s}\Gamma_\omega} \right) \sin \bar{\theta}, \\ T_\phi &= \frac{\sqrt{2}g_s}{3m_s} \frac{s}{m_\phi^2 - s - i\sqrt{s}\Gamma_\phi} \cos \bar{\theta}. \end{aligned} \quad (\text{A3})$$

It is worth noting that the amplitude with the intermediate photon (see Fig. 1) in this case can be easily combined with the amplitudes with the intermediate ρ , ω , and ϕ mesons [20]. At the result, we reproduce the vector-dominance model picture:

$$\begin{aligned}
 T_{\text{standard}} &= T_\gamma + T_{\rho+\omega} + T_\phi = T_{\rho+\omega}^{VMD} + T_\phi^{VMD}, \\
 T_{\rho+\omega}^{VMD} &= \frac{g_\pi}{2m_u} \left(3 \frac{1 - i\sqrt{s}\Gamma_\rho/m_\rho^2}{m_\rho^2 - s - i\sqrt{s}\Gamma_\rho} m_\rho^2 \right. \\
 &\quad \left. + \frac{1}{3} \frac{1 - i\sqrt{s}\Gamma_\omega/m_\omega^2}{m_\omega^2 - s - i\sqrt{s}\Gamma_\omega} m_\omega^2 \right) \sin \bar{\theta}, \quad (\text{A4}) \\
 T_\phi^{VMD} &= \frac{\sqrt{2}g_s}{3m_s} \frac{1 - i\sqrt{s}\Gamma_\phi/m_\phi^2}{m_\phi^2 - s - i\sqrt{s}\Gamma_\phi} m_\phi^2 \cos \bar{\theta}.
 \end{aligned}$$

One can see the comparison between the predictions given by the extended and standard versions of the NJL model in

TABLE II. Branching ratios for the processes $\rho \rightarrow \eta\gamma$, $\omega \rightarrow \eta\gamma$, and $\phi \rightarrow \eta\gamma$.

| Process | NJL | Experiment [13] | PDG [16] |
|--|-------|-------------------|------------------|
| $\mathcal{B}(\rho \rightarrow \eta\gamma) \times 10^4$ | 3.13 | 2.40 ± 0.32 | 3.00 ± 0.20 |
| $\mathcal{B}(\omega \rightarrow \eta\gamma) \times 10^4$ | 6.49 | 4.63 ± 0.59 | 4.6 ± 0.4 |
| $\mathcal{B}(\phi \rightarrow \eta\gamma) \times 10^4$ | 1.338 | 1.362 ± 0.054 | 1.309 ± 0.24 |

Figs. 3 and 4. Let us note that the standard NJL model gives us a value for the ϕ -resonance peak larger than the experimental value and the value predicted by the extended NJL model.

Using the formulas for the $V \rightarrow \eta\gamma$ vertices we can calculate the decay branching ratios for intermediate resonances into $\eta\gamma$ and compare them with experimental and PDG values. One can see a comparison in Table II.

-
- [1] E. A. Kuraev and M. K. Volkov, *Phys. Lett. B* **682**, 212 (2009).
 - [2] A. B. Arbuzov, E. A. Kuraev, and M. K. Volkov, *Eur. Phys. J. A* **47**, 103 (2011).
 - [3] M. K. Volkov and D. G. Kostunin, *Phys. Rev. C* **86**, 025202 (2012).
 - [4] A. B. Arbuzov, E. A. Kuraev, and M. K. Volkov, *Phys. Rev. C* **83**, 048201 (2011).
 - [5] A. I. Ahmadov, E. A. Kuraev, and M. K. Volkov, *Phys. Part. Nucl. Lett.* **9**, 461 (2012).
 - [6] M. K. Volkov and C. Weiss, *Phys. Rev. D* **56**, 221 (1997).
 - [7] M. K. Volkov, *Phys. Atom. Nucl.* **60**, 1920 (1997) [*Yad. Fiz.* **60**, 1094 (1997)].
 - [8] M. K. Volkov and A. E. Radzhabov, *Phys. Usp.* **49**, 551 (2006).
 - [9] S. I. Dolinsky, V. P. Druzhinin, M. S. Dubrovin *et al.*, *Phys. Rep.* **202**, 99 (1991).
 - [10] N. N. Achasov and A. A. Kozhevnikov, *Int. J. Mod. Phys. A* **7**, 4825 (1992).
 - [11] A. B. Arbuzov and M. K. Volkov, *Phys. Rev. C* **84**, 058201 (2011).
 - [12] M. K. Volkov and V. L. Yudichev, *Phys. Atom. Nucl.* **63**, 455 (2000) [*Yad. Fiz.* **63**, 527 (2000)].
 - [13] M. N. Achasov *et al.*, *Phys. Rev. D* **74**, 014016 (2006).
 - [14] M. K. Volkov, D. Ebert, and M. Nagy, *Int. J. Mod. Phys. A* **13**, 5443 (1998).
 - [15] M. K. Volkov and V. L. Yudichev, *Int. J. Mod. Phys. A* **14**, 4621 (1999).
 - [16] K. Nakamura *et al.* (Particle Data Group), *J. Phys. G* **37**, 075021 (2010).
 - [17] J. A. Oller and E. Oset, *Nucl. Phys. A* **629**, 739 (1998).
 - [18] M. K. Volkov and D. G. Kostunin, *Phys. Rev. D* **86**, 013005 (2012).
 - [19] Y. P. Ivanov, A. A. Osipov, and M. K. Volkov, *Z. Phys. C* **49**, 563 (1991).
 - [20] M. K. Volkov, *Sov. J. Part. Nucl.* **17**, 186 (1986) [*Fiz. Elem. Chast. Atom. Yadra* **17**, 433 (1986)].
 - [21] M. K. Volkov, *Phys. Part. Nucl.* **24**, 35 (1993).
 - [22] D. Ebert, H. Reinhardt, and M. K. Volkov, *Prog. Part. Nucl. Phys.* **33**, 1 (1994).